A Lattice-Reduction Aided Detection by Combining LLL Algorithm and Gram-Schmidt Procedure

Tadashi Fujino, Shinjiro Wakazono†, Yusuke Sasaki, and Xuan Nam Tran‡
The University of Electro-Communications, Chofu-shi, Tokyo, 182-8585, Japan
E-mail: {fujino, yusuke1227}@ice.uec.ac.jp, shinjiro15@gmail.com, namtx@lqdtu.edu.vn

***Abstract*—This paper proposes an improved lattice-reduction aided (LRA) MMSE detection by combining the LLL algorithm and the Gram-Schmidt (GS) procedure. The proposed detection reduces the column vectors of the MIMO channel matrix using the LLL algorithm and the GS procedure to create mutually purely orthogonal column vectors of the reduced channel matrix. Then the decision boundary becomes the same as that for the ML detection. Compared to the conventional LRA MMSE detector, the proposed detector achieves much closer BER performances to those for the ML detector in both the 4×4 MIMO and the 8×8 MIMO systems.**

***Index Terms*— Gram-Schmidt orthogonalization, lattice-reduction, LLL algorithm, MIMO, MMSE, signal estimation.**

I. Introduction

Recently, the lattice-reduction (LR) aided (LRA) detection has been receiving attractive attention since it achieves high channel capacity in the multiple-input multiple-output (MIMO) systems. The LR transforms the column vectors of the MIMO channel matrix close to mutually orthogonal, followed by the estimation of the transmitted signals [2]–[7]. The most popular LR algorithm is the well-known LLL algorithm introduced by Lenstra, Lenstra, and Lovász [1]. Using this algorithm, the LRA detector achieves highly reliable signal estimation and hence good bit error ratios (BERs). In particular, the LRA detector in a 4×4 MIMO system achieves BER relatively close to that with the maximum likelihood (ML) detector [2]–[5], [9], [10]. In contrast, the LRA detector in an 8×8 MIMO system does not achieve so good BER performance as the LRA detector in a 4×4 MIMO system does, compared to BERs for the ML detector [4], [9], [10]. This is because the signal transmitted from each antenna is interfered by more signals transmitted from the other antennas in the 8×8 MIMO system than in the 4×4 MIMO system. This fact implies that the detection scheme used for the 4×4 MIMO system is not directly applicable to the 8×8 MIMO system and that some adequate detection schemes should be needed for the 8×8 MIMO system.

In [9], we previously proposed a "combined forward and backward LR (F-LR and B-LR) aided detection scheme." This scheme improved the BER performance by around 3dB at BER≈10^{-5} over that with the conventional LRA detection in the 8×8 MIMO system. But the BER performance was still far from that with the ML detection.

In this paper, we propose an LRA minimum mean square error (MMSE) detection scheme by combining the LLL algorithm and the Gram-Schmidt (GS) orthogonalization procedure, aiming at achieving BER close to the BER for the ML detection in the 8×8 MIMO system. We first reduce the column vectors of the basis channel matrix using the LLL algorithm, and then reduce the LLL-reduced column vectors using the GS procedure. Then the GS-reduced column vectors become mutually purely orthogonal and almost of equal length. Hence the decision boundary becomes the same as that for the ML detection. As a result, the proposed detection scheme extremely improves the BER performance, which is very close to that with the ML detection both in the 4×4 and the 8×8 MIMO systems.

The remainder of this paper is organized as follows. Section II presents the system model and the conventional LRA detection. Section III presents the basic concept of the GS procedure based lattice-reduction. In Section IV, we propose a GS procedure based LRA MMSE detection which is applicable to the 8×8 MIMO systems. Section V gives the computer simulation results and makes discussion. Finally, we summarize and conclude the paper in Section VI.

II. System Model and Conventional LRA Detection

A. System Model

A MIMO system with M transmit and N ($N \geq M$) receive antennas is investigated here. In the system, the signals are transmitted over a rich scattering flat fading channel. We assume that the receiver has perfect knowledge of the channel state information. Let $\mathbf{H}=[\mathbf{h}_1,\ldots,\mathbf{h}_M]$ be the basis channel matrix, of which the entry $h_{n,m}$: $n\in[1,N]$, $m\in[1,M]$, at the n-th row and the m-th column is the complex channel gain between the m-th transmit and the n-th receive antennas. The channel gains are assumed to be mutually uncorrelated and of the complex Gaussian process with zero mean and unity variance. Let z_n be the additive noise at the n-th receiver, where z_n's: $n\in[1,N]$, are mutually uncorrelated. Each z_n is assumed to be of the complex Gaussian process with zero mean and variance of N_0, where N_0 is the one-sided noise power spectral density. Let $\mathbf{s}=[s_1,\ldots,s_M]^{\mathrm{T}}$, $\mathbf{y}=[y_1,\ldots,y_N]^{\mathrm{T}}$, and $\mathbf{z}=[z_1,\ldots,z_N]^{\mathrm{T}}$ be the transmit signal, receive signal, and the additive noise vectors, respectively. Then we have

$$\mathbf{y} = \mathbf{H}\mathbf{s} + \mathbf{z} = \mathbf{h}_1 s_1 + \mathbf{h}_2 s_2 + \cdots + \mathbf{h}_M s_M + \mathbf{z} \qquad (1)$$

B. LLL Algorithm

The most popular LRA detector employs the LLL algorithm shown in Table I. In the table, the optimum value of δ in terms of achieving low BER is dependent on the MIMO size and the modulation order, and on E_b/N_0 for MMSE. We will determine the value of δ in Section V. The operator $\lceil x \rfloor$ denotes the

† S. Wakazono is now with Sony Corporation, Tokyo, Japan. ‡ X. N. Tran is now with Le Qui Don Technical University, Hanoi, Vietnam.

rounding of x in the real and the imaginary parts separately. The algorithm transforms the basis channel matrix $\mathbf{H}$ to the reduced channel matrix $\mathbf{H}'$ and creates the transform matrix $\mathbf{T}$. The column vectors of $\mathbf{H}'$ are nearly orthogonal to one another, and $\mathbf{T}$ is a unimodular matrix with $\det\{\mathbf{T}\}=\pm 1$. Using $\mathbf{H}'$ and $\mathbf{T}$, eq. (1) is rewritten as

$$\mathbf{y} = \mathbf{H}\mathbf{s} + \mathbf{z} = (\mathbf{H}\mathbf{T})(\mathbf{T}^{-1}\mathbf{s}) + \mathbf{z} \equiv \mathbf{H}'\mathbf{v} + \mathbf{z} \tag{2}$$

where $\mathbf{H}'=\mathbf{H}\mathbf{T}$ and $\mathbf{v}=\mathbf{T}^{-1}\mathbf{s}$.

TABLE I
THE LLL ALGORITHM

(1) **Begin** Input $\mathbf{H}$, $\mathbf{T}:=\mathbf{I}_M=[\mathbf{t}_1,\ldots,\mathbf{t}_M]$, set δ, $\hat{\mathbf{h}}_1 = \mathbf{h}_1$
(2) **for** p:=2 to M
(3) **for** q:=p−1 down to 1
(4) $\mu_{p,q} = \hat{\mathbf{h}}_q^{\mathrm{H}}\mathbf{h}_p / \|\hat{\mathbf{h}}_q\|^2$
(5) $\mathbf{h}_p := \mathbf{h}_p - \lceil \mu_{p,q} \rfloor \mathbf{h}_q$, $\mathbf{t}_p := \mathbf{t}_p - \lceil \mu_{p,q} \rfloor \mathbf{t}_q$
(6) **end**
(7) Let $\hat{\mathbf{h}}_p = \mathbf{h}_p$.
(8) **for** q:=p−1 down to 1
(9) $\mu_{p,q} = \hat{\mathbf{h}}_q^{\mathrm{H}}\hat{\mathbf{h}}_p / \|\hat{\mathbf{h}}_q\|^2$
(10) $\hat{\mathbf{h}}_p := \hat{\mathbf{h}}_p - \mu_{p,q}\hat{\mathbf{h}}_q$
(11) **end**
(12) **If** $\delta \|\hat{\mathbf{h}}_{p-1}\|^2 \le \|\hat{\mathbf{h}}_p + \mu_{p,p-1}\hat{\mathbf{h}}_{p-1}\|^2$, let p:=p+1.
(13) **Else**, swap the (p−1)-th and the p-th columns.
Let p:=max{p−1, 2}, and $\hat{\mathbf{h}}_1 = \mathbf{h}_2$ if p=2.
(14) **end**
(15) **End**

For the MMSE estimation, following Hassibi [8], define the extended receive signal vector $\bar{\mathbf{y}}$, the extended channel matrix $\bar{\mathbf{H}}$, and the extended additive noise vector $\bar{\mathbf{z}}$, respectively, as

$$\bar{\mathbf{y}} \triangleq \begin{bmatrix} \mathbf{y} \\ \mathbf{0}_M \end{bmatrix},\ \bar{\mathbf{H}} \triangleq \begin{bmatrix} \mathbf{H} \\ \sqrt{\rho}\,\mathbf{I}_M \end{bmatrix},\ \bar{\mathbf{z}} \triangleq \begin{bmatrix} \mathbf{z} \\ -\sqrt{\rho}\,\mathbf{s} \end{bmatrix} \tag{3}$$

where $1/\rho=E_s/MN_0$ and $E_s=\mathrm{E}[|s_m|^2]$: $m\in[1,M]$. Here $\mathrm{E}[\cdot]$ is the ensemble average operator. The $\mathbf{I}_M$ is the $M\times M$ identity matrix, and $\mathbf{0}_M$ is the $M\times 1$ vector with all zero entries. Then input $\bar{\mathbf{H}}$ instead of $\mathbf{H}$ into step (1) of Table I. The column vectors $\bar{\mathbf{h}}_p$: $p\in[1,M]$, of $\bar{\mathbf{H}}$ are reduced to create the reduced channel matrix $\bar{\mathbf{H}}'$ and the transform matrix $\mathbf{T}$. Using $\bar{\mathbf{H}}'$ and $\mathbf{T}$, eq. (2) is extended as

$$\bar{\mathbf{y}} = \bar{\mathbf{H}}\mathbf{s} + \bar{\mathbf{z}} = (\bar{\mathbf{H}}\mathbf{T})(\mathbf{T}^{-1}\mathbf{s}) + \bar{\mathbf{z}} \equiv \bar{\mathbf{H}}'\mathbf{v} + \bar{\mathbf{z}} \tag{4}$$

where $\bar{\mathbf{H}}' = \bar{\mathbf{H}}\mathbf{T}$ and $\mathbf{v}=\mathbf{T}^{-1}\mathbf{s}$. Note that $\mathbf{T}$ and $\mathbf{v}$ in (4) are different from those in (2).

C. Estimation of Transmitted Signal

For the MIMO detection, the MMSE estimation is popular. In [8], Hassibi proposed a zero-forcing (ZF) similar form of the MMSE detector with introduction of $\bar{\mathbf{y}}$ and $\bar{\mathbf{H}}$ in (3). Then the MMSE estimation can be expressed in the similar form to the ZF as

$$\tilde{\mathbf{s}} = \bar{\mathbf{H}}^{\dagger}\bar{\mathbf{y}} = (\mathbf{H}^{\mathrm{H}}\mathbf{H} + \rho\,\mathbf{I}_M)^{-1}\mathbf{H}^{\mathrm{H}}\mathbf{y} \tag{5}$$

where $\bar{\mathbf{H}}^{\dagger}$ denotes the pseudo inverse of $\bar{\mathbf{H}}$. Then, $\tilde{\mathbf{s}}$ is transformed to $\tilde{\mathbf{v}} = \mathbf{T}^{-1}\tilde{\mathbf{s}}$ in the $\mathbf{v}$-domain. In the case that the entries of $\mathbf{s}$ are of the commonly used quadrature amplitude modulation (QAM) mapping, proper shifting and scaling of $\tilde{\mathbf{s}}$ is necessary before deriving $\tilde{\mathbf{v}}$. The detailed explanation on the shifting and scaling operation is given in [7]. We express this operation as $\tilde{\mathbf{s}} := \mathcal{S}[\tilde{\mathbf{s}}]$. After that, the entries of $\tilde{\mathbf{v}}$ are rounded as $\hat{\mathbf{v}} = \lceil \tilde{\mathbf{v}} \rfloor$. Next, $\hat{\mathbf{v}}$ is transformed to $\hat{\mathbf{s}} = \mathbf{T}\hat{\mathbf{v}}$ in the $\mathbf{s}$-domain. Then, $\hat{\mathbf{s}}$ is shifted back and scaled back in the above case. We express this operation as $\hat{\mathbf{s}} := \mathcal{S}^{-1}[\hat{\mathbf{s}}]$. At this stage, entries $\hat{s}_m$: $m\in[1,M]$, of $\hat{\mathbf{s}}$ are forced to the nearest symbol constellation point if they are lying outside the symbol constellation. We express this operation as $\hat{\mathbf{s}} := \mathcal{C}[\hat{\mathbf{s}}]$.

III. BASIC CONCEPT OF GRAM-SCHMIDT PROCEDURE BASED LRA MMSE DETECTION

In this section, the basic concept of the proposed GS procedure based LRA MMSE detection is explained shortly. The LLL algorithm transforms the extended basis channel matrix $\bar{\mathbf{H}}$ to the reduced channel matrix $\bar{\mathbf{H}}'$, of which the column vectors are mutually nearly orthogonal. The algorithm also makes the reduced column vectors almost of equal length. If the reduced column vectors were mutually purely orthogonal, the decision boundary for the receive signal should be the same as that for the ML detection. Unfortunately, the LLL algorithm does not make the column vectors of the reduced channel matrix $\bar{\mathbf{H}}'$ mutually purely orthogonal. Hence we will make them purely orthogonal using the GS procedure, as described below.

Table II shows a GS orthogonalization algorithm. This algorithm weakly reduces the column vectors of the LLL-reduced channel matrix $\mathbf{H}'$ to create the GS-reduced channel matrix $\hat{\mathbf{H}}$ and the transform matrix $\hat{\mathbf{T}}$. The column vectors of $\hat{\mathbf{H}}$ are mutually purely orthogonal. Note that the algorithm in Table II is computationally-simple since it weakly reduces the column vectors of $\mathbf{H}'$.

TABLE II
GRAM-SCHMIDT ORTHGONALIZATION ALGORITHM

(1) **Begin** Input $\mathbf{H}' = [\mathbf{h}'_1,\ldots,\mathbf{h}'_M]$, $\hat{\mathbf{T}} := \mathbf{I}_M = [\mathbf{t}_1,\ldots,\mathbf{t}_M]$,
set $\hat{\mathbf{h}}_p = \mathbf{h}'_p$, $\hat{\mathbf{t}}_p = \mathbf{t}_p : p\in[1,M]$
(2) **for** p:=2 to M
(3) **for** q:=p−1 down to 1
(4) $\mu_{p,q} = \hat{\mathbf{h}}_q^{\mathrm{H}}\hat{\mathbf{h}}_p / \|\hat{\mathbf{h}}_q\|^2$
(5) $\hat{\mathbf{h}}_p := \hat{\mathbf{h}}_p - \mu_{p,q}\hat{\mathbf{h}}_q$, $\hat{\mathbf{t}}_p := \hat{\mathbf{t}}_p - \mu_{p,q}\hat{\mathbf{t}}_q$
(6) **end**
(7) **end**
(8) **End**

For MMSE, the column vectors of $\bar{\mathbf{H}}'$ are weakly reduced using Table II to create the GS-reduced channel matrix $\hat{\bar{\mathbf{H}}}$ and the transform matrix $\hat{\mathbf{T}}$. Extending (4), we have

$$\begin{aligned} \bar{\mathbf{y}} &= \bar{\mathbf{H}}\mathbf{s} + \bar{\mathbf{z}} = (\bar{\mathbf{H}}\mathbf{T})(\mathbf{T}^{-1}\mathbf{s}) + \bar{\mathbf{z}} \equiv \bar{\mathbf{H}}'\mathbf{v} + \bar{\mathbf{z}} \\ &= (\bar{\mathbf{H}}'\hat{\mathbf{T}})(\hat{\mathbf{T}}^{-1}\mathbf{v}) + \bar{\mathbf{z}} \equiv \hat{\bar{\mathbf{H}}}\mathbf{u} + \bar{\mathbf{z}} \end{aligned} \tag{6}$$

where $\hat{\bar{\mathbf{H}}} = \bar{\mathbf{H}}'\hat{\mathbf{T}} = \bar{\mathbf{H}}\mathbf{T}\hat{\mathbf{T}}$, $\mathbf{s} = \mathbf{T}\mathbf{v} = \mathbf{T}\hat{\mathbf{T}}\mathbf{u}$, and $\det\{\mathbf{T}\hat{\mathbf{T}}\} = \pm 1$. Note that $\hat{\mathbf{T}}$ is an upper triangular matrix with unity diagonal entries and the others of non-integers.

The soft estimate of $\mathbf{u}$ is expressed as $\tilde{\mathbf{u}} = (\mathbf{T}\hat{\mathbf{T}})^{-1}\tilde{\mathbf{s}}$. Since the entries of $\mathbf{u}\,(=(\mathbf{T}\hat{\mathbf{T}})^{-1}\mathbf{s})$ are not integers, the entries of $\tilde{\mathbf{u}}$ cannot be decided by quantization like the LRA detection. A most critical problem for the proposed detection is how to decide $\tilde{\mathbf{u}}$ to create the estimate $\hat{\mathbf{u}}$ in the $\mathbf{u}$-domain. This problem will be uniquely solved using a novel method in Section IV. Once $\tilde{\mathbf{u}}$ is decided to be $\hat{\mathbf{u}}$, the estimate of the transmitted signal $\mathbf{s}$ is obtained as $\hat{\mathbf{s}} = \mathbf{T}\hat{\mathbf{T}}\hat{\mathbf{u}}$, and then let $\hat{\mathbf{s}} := \mathcal{S}^{-1}[\hat{\mathbf{s}}]$ and

$\hat{\mathbf{s}} := \mathcal{C}[\hat{\mathbf{s}}]$.

IV. Proposed LRA MMSE Detection Based on Gram-Schmidt Procedure

In this section, the detailed procedure of the proposed GS-based LRA MMSE detection is explained.

A. Forward and Backward LR Using LLL Algorithm

(i) First we forward reduce the column vectors of $\overline{\mathbf{H}} = [\overline{\mathbf{h}}_1, ..., \overline{\mathbf{h}}_M]$ using Table I. Input $\mathbf{H} = [\mathbf{h}_1, ..., \mathbf{h}_M] := \overline{\mathbf{H}}$ and $\mathbf{T} := \mathbf{I}_M = [\mathbf{t}_1, \ldots, \mathbf{t}_M]$ into Table I. Then we obtain the LLL-reduced channel matrix $\overline{\mathbf{H}}'^{(j=1)} \equiv [\overline{\mathbf{h}}_1'^{(j=1)}, ..., \overline{\mathbf{h}}_M'^{(j=1)}] := [\mathbf{h}_1, ..., \mathbf{h}_M]$ and the transform matrix $\mathbf{T}^{(j=1)} \equiv [\mathbf{t}_1^{(j=1)}, ..., \mathbf{t}_M^{(j=1)}] := [\mathbf{t}_1, ..., \mathbf{t}_M]$.

Next we backward reduce the column vectors of $\overline{\mathbf{H}}$ using Table I. Input $\mathbf{H} = [\mathbf{h}_1, ..., \mathbf{h}_M] := [\overline{\mathbf{h}}_M, ..., \overline{\mathbf{h}}_1]$ and $\mathbf{T} = [\mathbf{t}_1, \ldots, \mathbf{t}_M] := [\mathbf{t}_M, \ldots, \mathbf{t}_1]$ into Table I. Then we obtain the LLL-reduced channel matrix $\overline{\mathbf{H}}'^{(j=2)} \equiv [\overline{\mathbf{h}}_1'^{(j=2)}, ..., \overline{\mathbf{h}}_M'^{(j=2)}] := [\mathbf{h}_M, ..., \mathbf{h}_1]$ and the transform matrix $\mathbf{T}^{(j=2)} \equiv [\mathbf{t}_1^{(j=2)}, ..., \mathbf{t}_M^{(j=2)}] := [\mathbf{t}_M, ..., \mathbf{t}_1]$.

(ii) If we want better BER, we further rearrange the order of the columns of $\overline{\mathbf{H}}$ and of $\mathbf{T}$ such that

$\mathbf{H} = [\mathbf{h}_1, ..., \mathbf{h}_M] := [\overline{\mathbf{h}}_{M/2+1}, ..., \overline{\mathbf{h}}_M, \overline{\mathbf{h}}_1, ..., \overline{\mathbf{h}}_{M/2}]$

$\mathbf{T} = [\mathbf{t}_1, ..., \mathbf{t}_M] := [\mathbf{t}_{M/2+1}, ..., \mathbf{t}_M, \mathbf{t}_1, ..., \mathbf{t}_{M/2}]$

for the forward LLL-reduction, and

$\mathbf{H} = [\mathbf{h}_1, ..., \mathbf{h}_M] := [\overline{\mathbf{h}}_{M/2}, ..., \overline{\mathbf{h}}_1, \overline{\mathbf{h}}_M, ..., \overline{\mathbf{h}}_{M/2+1}]$

$\mathbf{T} = [\mathbf{t}_1, ..., \mathbf{t}_M] := [\mathbf{t}_{M/2}, ..., \mathbf{t}_1, \mathbf{t}_M, ..., \mathbf{t}_{M/2+1}]$

for the backward LLL-reduction.

Input the above $\mathbf{H}$'s and $\mathbf{T}$'s into Table I. Then we obtain the LLL-reduced channel matrices and the transform matrices as

$\overline{\mathbf{H}}'^{(j=3)} \equiv [\overline{\mathbf{h}}_1'^{(j=3)}, ..., \overline{\mathbf{h}}_M'^{(j=3)}] := [\mathbf{h}_{M/2+1}, ..., \mathbf{h}_M, \mathbf{h}_1, ..., \mathbf{h}_{M/2}]$

$\mathbf{T}^{(j=3)} \equiv [\mathbf{t}_1^{(j=3)}, ..., \mathbf{t}_M^{(j=3)}] := [\mathbf{t}_{M/2+1}, ..., \mathbf{t}_M, \mathbf{t}_1, ..., \mathbf{t}_{M/2}]$

and

$\overline{\mathbf{H}}'^{(j=4)} \equiv [\overline{\mathbf{h}}_1'^{(j=4)}, ..., \overline{\mathbf{h}}_M'^{(j=4)}] := [\mathbf{h}_{M/2}, ..., \mathbf{h}_1, \mathbf{h}_M, ..., \mathbf{h}_{M/2+1}]$

$\mathbf{T}^{(j=4)} \equiv [\mathbf{t}_1^{(j=4)}, ..., \mathbf{t}_M^{(j=4)}] := [\mathbf{t}_{M/2}, ..., \mathbf{t}_1, \mathbf{t}_M, ..., \mathbf{t}_{M/2+1}]$.

In (i), the superscripts (j=1) and (j=2) denote the F-LR and the B-LR of the extended channel matrix $\overline{\mathbf{H}}$, respectively. In (ii), the superscripts (j=3) and (j=4) denote the F-LR and the B-LR of the column-order rearranged $\overline{\mathbf{H}}$, respectively.

B. Gram-Schmidt Orthogonalization

We next create eight or 16 GS-reduced channel matrices $\hat{\overline{\mathbf{H}}}$'s and their corresponding transform matrices $\hat{\mathbf{T}}$'s by inputting $\overline{\mathbf{H}}'^{(j)}: j \in \{1,2\}$ or $j \in [1,4]$, into Table II.

Case 1 (k=1)**:** Forward GS-reduction of $\overline{\mathbf{H}}'^{(j)}$:

Input the LLL-reduced channel matrix

$\mathbf{H}' = [\mathbf{h}_1', ..., \mathbf{h}_M'] := [\overline{\mathbf{h}}_1'^{(j)}, ..., \overline{\mathbf{h}}_M'^{(j)}] = \overline{\mathbf{H}}'^{(j)}$ and

$\hat{\mathbf{T}} = [\mathbf{t}_1, ..., \mathbf{t}_M] := \mathbf{I}_M$.

Then we obtain the GS-reduced channel matrix

$\hat{\overline{\mathbf{H}}}^{(j,k=1)} \equiv [\hat{\overline{\mathbf{h}}}_1^{(j,k=1)}, ..., \hat{\overline{\mathbf{h}}}_M^{(j,k=1)}] := [\hat{\mathbf{h}}_1, ..., \hat{\mathbf{h}}_M]$

and the transform matrix

$\hat{\mathbf{T}}^{(j,k=1)} \equiv [\hat{\mathbf{t}}_1^{(j,k=1)}, ..., \hat{\mathbf{t}}_M^{(j,k=1)}] := [\hat{\mathbf{t}}_1, ..., \hat{\mathbf{t}}_M]$.

Case 2 (k=2)**:** Backward GS-reduction of $\overline{\mathbf{H}}'^{(j)}$:

Input

$\mathbf{H}' = [\mathbf{h}_1', ..., \mathbf{h}_M'] := [\overline{\mathbf{h}}_M'^{(j)}, ..., \overline{\mathbf{h}}_1'^{(j)}]$ and

$\hat{\mathbf{T}} = [\mathbf{t}_1, ..., \mathbf{t}_M] := [\mathbf{t}_M, ..., \mathbf{t}_1]$.

Then we obtain

$\hat{\overline{\mathbf{H}}}^{(j,k=2)} \equiv [\hat{\overline{\mathbf{h}}}_1^{(j,k=2)}, ..., \hat{\overline{\mathbf{h}}}_M^{(j,k=2)}] := [\hat{\mathbf{h}}_M, ..., \hat{\mathbf{h}}_1]$ and

$\hat{\mathbf{T}}^{(j,k=2)} \equiv [\hat{\mathbf{t}}_1^{(j,k=2)}, ..., \hat{\mathbf{t}}_M^{(j,k=2)}] := [\hat{\mathbf{t}}_M, ..., \hat{\mathbf{t}}_1]$.

Case 3 (k=3)**:** Forward GS-reduction of the column-order rearranged $\overline{\mathbf{H}}'^{(j)}$:

Input

$\mathbf{H}' = [\mathbf{h}_1', ..., \mathbf{h}_M'] := [\overline{\mathbf{h}}_{M/2+1}'^{(j)}, ..., \overline{\mathbf{h}}_M'^{(j)}, \overline{\mathbf{h}}_1'^{(j)}, ..., \overline{\mathbf{h}}_{M/2}'^{(j)}]$ and

$\hat{\mathbf{T}} = [\mathbf{t}_1, ..., \mathbf{t}_M] := [\mathbf{t}_{M/2+1}, ..., \mathbf{t}_M, \mathbf{t}_1, ..., \mathbf{t}_{M/2}]$.

Then we obtain

$\hat{\overline{\mathbf{H}}}^{(j,k=3)} \equiv [\hat{\overline{\mathbf{h}}}_1^{(j,k=3)}, ..., \hat{\overline{\mathbf{h}}}_M^{(j,k=3)}] := [\hat{\mathbf{h}}_{M/2+1}, ..., \hat{\mathbf{h}}_M, \hat{\mathbf{h}}_1, ..., \hat{\mathbf{h}}_{M/2}]$

and

$\hat{\mathbf{T}}^{(j,k=3)} \equiv [\hat{\mathbf{t}}_1^{(j,k=3)}, ..., \hat{\mathbf{t}}_M^{(j,k=3)}] := [\hat{\mathbf{t}}_{M/2+1}, ..., \hat{\mathbf{t}}_M, \hat{\mathbf{t}}_1, ..., \hat{\mathbf{t}}_{M/2}]$.

Case 4 (k=4)**:** Backward GS-reduction of the column-order rearranged $\overline{\mathbf{H}}'^{(j)}$:

Input

$\mathbf{H}' = [\mathbf{h}_1', ..., \mathbf{h}_M'] := [\overline{\mathbf{h}}_{M/2}'^{(j)}, ..., \overline{\mathbf{h}}_1'^{(j)}, \overline{\mathbf{h}}_M'^{(j)}, ..., \overline{\mathbf{h}}_{M/2+1}'^{(j)}]$ and

$\hat{\mathbf{T}} = [\mathbf{t}_1, ..., \mathbf{t}_M] := [\mathbf{t}_{M/2}, ..., \mathbf{t}_1, \mathbf{t}_M, ..., \mathbf{t}_{M/2+1}]$.

Then we obtain

$\hat{\overline{\mathbf{H}}}^{(j,k=4)} \equiv [\hat{\overline{\mathbf{h}}}_1^{(j,k=4)}, ..., \hat{\overline{\mathbf{h}}}_M^{(j,k=4)}] := [\hat{\mathbf{h}}_{M/2}, ..., \hat{\mathbf{h}}_1, \hat{\mathbf{h}}_M, ..., \hat{\mathbf{h}}_{M/2+1}]$

and

$\hat{\mathbf{T}}^{(j,k=4)} \equiv [\hat{\mathbf{t}}_1^{(j,k=4)}, ..., \hat{\mathbf{t}}_M^{(j,k=4)}] := [\hat{\mathbf{t}}_{M/2}, ..., \hat{\mathbf{t}}_1, \hat{\mathbf{t}}_M, ..., \hat{\mathbf{t}}_{M/2+1}]$.

In the above Cases 1–4, the superscripts (k=1) and (k=2) denote the forward and the backward GS-reductions of $\overline{\mathbf{H}}'^{(j)}$, respectively, and the superscripts (k=3) and (k=4) denote the forward and the backward GS-reductions of the column-order rearranged $\overline{\mathbf{H}}'^{(j)}$, respectively.

Finally, the extended receive signal vector $\overline{\mathbf{y}}$ is obtained as

$$\begin{aligned}\overline{\mathbf{y}} &= \overline{\mathbf{H}}\mathbf{s} + \overline{\mathbf{z}} = (\overline{\mathbf{H}}\mathbf{T}^{(j)})(\mathbf{T}^{(j)-1}\mathbf{s}) + \overline{\mathbf{z}} \equiv \overline{\mathbf{H}}'^{(j)}\mathbf{v}^{(j)} + \overline{\mathbf{z}} \\ &= (\overline{\mathbf{H}}'^{(j)}\hat{\mathbf{T}}^{(j,k)})(\hat{\mathbf{T}}^{(j,k)-1}\mathbf{v}^{(j)}) + \overline{\mathbf{z}} \\ &\equiv (\overline{\mathbf{H}}\hat{\underset{\sim}{\mathbf{T}}}^{(j,k)})(\hat{\underset{\sim}{\mathbf{T}}}^{(j,k)-1}\mathbf{s}) + \overline{\mathbf{z}} \equiv \hat{\overline{\mathbf{H}}}^{(j,k)}\mathbf{u}^{(j,k)} + \overline{\mathbf{z}}\end{aligned} \tag{7}$$

where ($j \in \{1,2\}$ or $j \in [1,4]$), $k \in [1,4]$, $\hat{\underset{\sim}{\mathbf{T}}}^{(j,k)} \triangleq \mathbf{T}^{(j)}\hat{\mathbf{T}}^{(j,k)}$, $\hat{\overline{\mathbf{H}}}^{(j,k)} = \overline{\mathbf{H}}'^{(j)}\hat{\mathbf{T}}^{(j,k)} = \overline{\mathbf{H}}\hat{\underset{\sim}{\mathbf{T}}}^{(j,k)}$, and

$$\mathbf{s} = \mathbf{T}^{(j)}\mathbf{v}^{(j)} = \hat{\underset{\sim}{\mathbf{T}}}^{(j,k)}\mathbf{u}^{(j,k)} \tag{8}$$

Note that the entries of $\hat{\underset{\sim}{\mathbf{T}}}^{(j,k)}$ and of $\mathbf{u}^{(j,k)}$ are not integers, and $\det\{\hat{\underset{\sim}{\mathbf{T}}}^{(j,k)}\} = \pm 1$.

C. Estimation of Signal Vector $\mathbf{u}$

The transmitted signal $\mathbf{s}$ in (8) is first shifted and scaled as $\mathbf{s} := \mathcal{S}[\mathbf{s}]$. Then it is transformed to $\mathbf{u}^{(j,k)}$ as

$$\mathbf{u}^{(j,k)} = [u_1^{(j,k)}, ..., u_M^{(j,k)}]^{\mathrm{T}} = \hat{\underset{\sim}{\mathbf{T}}}^{(j,k)-1}\mathbf{s} \tag{9}$$

where ($j \in \{1,2\}$ or $j \in [1,4]$) and $k \in [1,4]$. Then we measure the distance between $\mathbf{u}^{(j,k)}$ and the origin $\mathbf{0}_M$ as

$$\Delta\mathbf{u}^{(j,k)} = \mathbf{0}_M - \mathbf{u}^{(j,k)} = -\mathbf{u}^{(j,k)} = -\hat{\underset{\sim}{\mathbf{T}}}^{(j,k)-1}\mathbf{s} \tag{10}$$

The m-th entry of $\Delta\mathbf{u}^{(j,k)}$ is expressed as $\Delta u_m^{(j,k)} = -u_m^{(j,k)}$. After $\tilde{\mathbf{s}}$ in (5) is shifted and scaled as $\tilde{\mathbf{s}} := \mathcal{S}[\tilde{\mathbf{s}}]$, the soft estimate of $\mathbf{u}^{(j,k)}$ is derived from $\tilde{\mathbf{s}}$ as

$$\tilde{\mathbf{u}}^{(j,k)} = [\tilde{u}_1^{(j,k)}, ..., \tilde{u}_M^{(j,k)}]^{\mathrm{T}} = \hat{\underset{\sim}{\mathbf{T}}}^{(j,k)-1}\tilde{\mathbf{s}} \tag{11}$$

Now we have obtained the correct point $u_m^{(j,k)}$ in (9) and the soft estimate $\tilde{u}_m^{(j,k)}$ in (11). Since $u_m^{(j,k)}$ is not an integer, $\tilde{u}_m^{(j,k)}$ cannot be decided by quantization like the conventional LRA detector. In order to decide of $\tilde{u}_m^{(j,k)}$, we shift both $u_m^{(j,k)}$ and $\tilde{u}_m^{(j,k)}$ by $\Delta u_m^{(j,k)} (= -u_m^{(j,k)})$ such that $u_m^{(j,k)}$ should be

shifted to the origin. Then the shifted $u_m^{(j,k)}$ and $\tilde{u}_m^{(j,k)}$ are expressed, respectively, as

$$u_m'^{(j,k)} = u_m^{(j,k)} + \Delta u_m^{(j,k)} = u_m^{(j,k)} - u_m^{(j,k)} = 0 \quad (12)$$

$$\tilde{u}_m'^{(j,k)} = \tilde{u}_m^{(j,k)} + \Delta u_m^{(j,k)} = \tilde{u}_m^{(j,k)} - u_m^{(j,k)} \quad (13)$$

Since $u_m'^{(j,k)}$ is an integer (zero), $\tilde{u}_m'^{(j,k)}$ can be rounded as

$$\hat{u}_m'^{(j,k)} = \lceil \tilde{u}_m'^{(j,k)} \rfloor = \lceil \tilde{u}_m^{(j,k)} - u_m^{(j,k)} \rfloor \quad (14)$$

After that, shift back $\hat{u}_m'^{(j,k)}$ by $-\Delta u_m^{(j,k)} (= u_m^{(j,k)})$ to create the decided estimate $\hat{u}_m^{(j,k)}$ as

$$\hat{u}_m^{(j,k)} = \hat{u}_m'^{(j,k)} - \Delta u_m^{(j,k)} = \lceil \tilde{u}_m^{(j,k)} - u_m^{(j,k)} \rfloor + u_m^{(j,k)} \quad (15)$$

Using (9), eq. (15) is expressed in the vector form as

$$\hat{\mathbf{u}}^{(j,k)} = \hat{\mathbf{u}}'^{(j,k)} - \Delta\hat{\mathbf{u}}^{(j,k)} = \lceil \tilde{\mathbf{u}}^{(j,k)} - \hat{\underset{\sim}{\mathbf{T}}}^{(j,k)-1}\mathbf{s} \rfloor + \hat{\underset{\sim}{\mathbf{T}}}^{(j,k)-1}\mathbf{s} \quad (16)$$

We here pre-estimate the transmitted signal $\mathbf{s}$ in (16) using the conventional LRA MMSE detection. First, derive the soft estimate $\tilde{\mathbf{s}}$ in (5). Then let $\tilde{\mathbf{s}} := \mathcal{S}[\tilde{\mathbf{s}}]$. Next, transform $\tilde{\mathbf{s}}$ to $\tilde{\mathbf{v}}^{(j)} = \mathbf{T}^{(j)-1}\tilde{\mathbf{s}}$ in the $\mathbf{v}$-domain. Then, round the entries of $\tilde{\mathbf{v}}^{(j)}$ as $\hat{\mathbf{v}}^{(j)} = \lceil \tilde{\mathbf{v}}^{(j)} \rfloor$. Finally, transform $\hat{\mathbf{v}}^{(j)}$ to $\hat{\mathbf{s}}'^{(j)}$ in the $\mathbf{s}$-domain as

$$\hat{\mathbf{s}}'^{(j)} = \mathbf{T}^{(j)}\hat{\mathbf{v}}^{(j)} \quad (17)$$

Substitute $\hat{\mathbf{s}}'^{(j)}$ into $\mathbf{s}$ in (16) to revise $\hat{\mathbf{u}}^{(j,k)}$.

Note that the cross-correlation of $\mathbf{T}^{(j=1)}$ and $\mathbf{T}^{(j=2)}$ and that of $\mathbf{T}^{(j=3)}$ and $\mathbf{T}^{(j=4)}$ are weak as shown in [9]. Hence it is unlikely that all $\hat{\mathbf{s}}'^{(j)}: j\in[1,4]$, in (17) are in error at the same time. Similarly, the cross-correlation of $\hat{\underset{\sim}{\mathbf{T}}}^{(j,k)}$ and $\hat{\underset{\sim}{\mathbf{T}}}^{(j',k')}$ is weak, where $j' \neq j$ and/or $k' \neq k$. Hence it is unlikely that all $\hat{\mathbf{s}}^{(j,k)}$ $(= \hat{\underset{\sim}{\mathbf{T}}}^{(j,k)}\hat{\mathbf{u}}^{(j,k)}) : \{j|k\}\in[1,4]$, are in error at the same time. As a result, good BER should be expected by selecting the most reliable estimate $\hat{\mathbf{s}}^{(j,k)}$.

D. List of $\hat{\mathbf{u}}$ and Estimation of $\mathbf{s}$

We here derive the estimate of the transmitted signal $\mathbf{s}$ using the proposed GS-based LRA MMSE detection. Replacing $\mathbf{s}$ in (16) by $\hat{\mathbf{s}}'^{(j)}$ in (17), we express the revised $\hat{\mathbf{u}}^{(j,k)}$ as $\hat{\mathbf{u}}^{(p=0,j,k)}$, which is first listed. Since $\tilde{\mathbf{u}}^{(j,k)} \approx \mathbf{u}^{(j,k)}$ in the high E_b/N_0 region, we further create $\hat{\mathbf{u}}^{(p,j,k)}: p\in[1,M]$, by replacing the p-th entry of $\hat{\mathbf{u}}^{(0,j,k)}$ by $\tilde{u}_p^{(j,k)}$ in (11). And add them to the list. By adding $\hat{\mathbf{u}}^{(p,j,k)}: p\in[1,M]$, to the list, more reliable estimate of the transmitted signal $\mathbf{s}$ is expected. Calculating $\hat{\mathbf{s}}^{(p,j,k)} = \hat{\underset{\sim}{\mathbf{T}}}^{(j,k)}\hat{\mathbf{u}}^{(p,j,k)}$: $p\in[0,M]$, and then letting $\hat{\mathbf{s}}^{(p,j,k)} := \mathcal{S}^{-1}[\hat{\mathbf{s}}^{(p,j,k)}]$ and $\hat{\mathbf{s}}^{(p,j,k)} := \mathcal{C}[\hat{\mathbf{s}}^{(p,j,k)}]$, select the most reliable signal among all $\hat{\mathbf{s}}^{(p,j,k)}: p\in[0,M]$, ($j\in\{1,2\}$ or $j\in[1,4]$), $k\in[1,4]$. The above procedure is summarized in Table III, where the notations $\mathcal{S}[\cdot]$ and $\mathcal{S}^{-1}[\cdot]$ for $\hat{\mathbf{s}}^{(p,j,k)}$, $\hat{\mathbf{s}}^{[i,j,k]}$, $\hat{\mathbf{s}}'^{(j)}$ and $\hat{\mathbf{s}}'^{\{i\}}$ are omitted.

In Table III, we obtain the estimate $\hat{\mathbf{s}}$ at step (28). We here call the $\hat{\mathbf{s}}$ the GS-estimate. We also call this detection procedure *the Gram-Schmidt based combined forward and backward LRA (GS-F&B-LRA) MMSE list detection*. In order to achieve more reliable GS-estimate $\hat{\mathbf{s}}$, we replace $\hat{\mathbf{s}}'^{\{i\}}$ at step (6) by the updated estimate $\hat{\mathbf{s}}^{(p=M,j,k)}$ at step (15) for each j and k iteratively, where i is the iteration number and I is the number of iterations. Note that the "combined forward and backward (F&B) LRA detection scheme" is explained in [9].

In this section, the transmitted signal $\mathbf{s}$ is estimated in the following manner. First the extended channel matrix $\bar{\mathbf{H}}$ is forward and backward reduced using the LLL algorithm in Table I to create two or four reduced matrices $\bar{\mathbf{H}}'$'s. After that, eight or 16 $\hat{\bar{\mathbf{H}}}$'s are created by forward and backward reducing the column vectors of $\bar{\mathbf{H}}'$'s using the weakly reducing GS algorithm in Table II, followed by the estimation of the transmitted signal $\mathbf{s}$. With this procedure, all the columns of $\hat{\bar{\mathbf{H}}}$ become purely orthogonal to one another and almost of equal length. Hence good BER is expected.

TABLE III
THE PROPOSED DETECTION ALGORITHM

(1) **Begin** Input $\mathbf{y}$, $\tilde{\mathbf{u}}^{(j,k)} = [\tilde{u}_1^{(j,k)},...,\tilde{u}_M^{(j,k)}]^{\mathrm{T}}$, $\hat{\underset{\sim}{\mathbf{T}}}^{(j,k)}$, $\hat{\underset{\sim}{\mathbf{T}}}^{(j,k)-1}$, $\hat{\mathbf{s}}'^{(j)}$, $\mathbf{H}$.
(2) **for** j:=1 to (2 or 4)
(3) **for** k:=1 to 4
(4) Let $\hat{\mathbf{s}}'^{\{i=0\}} := \hat{\mathbf{s}}'^{(j)}$.
(5) **for** i:=0 to I (I: the number of iterations)
(6) $\hat{\mathbf{u}}^{(p=0,j,k)} = \lceil \tilde{\mathbf{u}}^{(j,k)} - \hat{\underset{\sim}{\mathbf{T}}}^{(j,k)-1}\hat{\mathbf{s}}'^{\{i\}} \rfloor + \hat{\underset{\sim}{\mathbf{T}}}^{(j,k)-1}\hat{\mathbf{s}}'^{\{i\}}$
(7) $\hat{\mathbf{s}}^{(p=0,j,k)} = \hat{\underset{\sim}{\mathbf{T}}}^{(j,k)}\hat{\mathbf{u}}^{(0,j,k)}$, and let $\hat{\mathbf{s}}^{(0,j,k)} := \mathcal{C}[\hat{\mathbf{s}}^{(0,j,k)}]$.
(8) **for** p:=1 to M
(9) $\hat{\mathbf{u}}^{(p,j,k)} = [...,\tilde{u}_p^{(j,k)},...,\hat{u}_q^{(j,k)},...]^{\mathrm{T}} : (q\neq p)\cap(q\in[1,M])$
(10) $\hat{\mathbf{s}}^{(p,j,k)} = \hat{\underset{\sim}{\mathbf{T}}}^{(j,k)}\hat{\mathbf{u}}^{(p,j,k)}$, and let $\hat{\mathbf{s}}^{(p,j,k)} := \mathcal{C}[\hat{\mathbf{s}}^{(p,j,k)}]$.
(11) **If** $\hat{\mathbf{s}}^{(p,j,k)} = \hat{\mathbf{s}}^{(p-1,j,k)}$, go to (13).
(12) **Else**, $\hat{\mathbf{s}}^{(p,j,k)} = \underset{p'\in\{p-1,p\}}{\arg\min} [\| \mathbf{y} - \mathbf{H}\hat{\mathbf{s}}^{(p',j,k)} \|]$.
(13) **end** (p-loop)
(14) Let $\hat{\mathbf{s}}^{[i,j,k]} := \hat{\mathbf{s}}^{(p=M,j,k)}$.
(15) Let $\hat{\mathbf{s}}'^{\{i\}} := \hat{\mathbf{s}}^{(p=M,j,k)}$.
(16) **If** i=0, go to (19).
(17) **If** $\hat{\mathbf{s}}'^{\{i\}} = \hat{\mathbf{s}}'^{\{i'\}}$ for any one of i': $i'\in[0,i-1]$, then let $\hat{\mathbf{s}}^{[I,j,k]} := \hat{\mathbf{s}}^{[i,j,k]}$, and go to (20).
(18) **Else**, let $\hat{\mathbf{s}}^{[i,j,k]} := \underset{i'\in\{i-1,i\}}{\arg\min}[\| \mathbf{y} - \mathbf{H}\hat{\mathbf{s}}^{[i',j,k]} \|]$.
(19) **end** (i-loop)
(20) **If** k=1, go to (23).
(21) **If** $\hat{\mathbf{s}}^{[i=I,j,k]} = \hat{\mathbf{s}}^{[i=I,j,k-1]}$, go to (23).
(22) **Else**, $\hat{\mathbf{s}}^{[i=I,j,k]} := \underset{k'\in\{k-1,k\}}{\arg\min} [\| \mathbf{y} - \mathbf{H}\hat{\mathbf{s}}^{[i=I,j,k']} \|]$.
(23) **end** (k-loop)
(24) **If** j=1, go to (27).
(25) **If** $\hat{\mathbf{s}}^{[i=I,j,k=4]} = \hat{\mathbf{s}}^{[i=I,j-1,k=4]}$, go to (27).
(26) **Else**, $\hat{\mathbf{s}}^{[i=I,j,k=4]} := \underset{j'\in\{j-1,j\}}{\arg\min} [\| \mathbf{y} - \mathbf{H}\hat{\mathbf{s}}^{[i=I,j',k=4]} \|]$.
(27) **end** (j-loop)
(28) Let $\hat{\mathbf{s}} = \hat{\mathbf{s}}^{[i=I,(j=2 \text{ or } 4),k=4]}$ and let $\hat{\mathbf{s}} := \mathcal{C}[\hat{\mathbf{s}}]$. (GS-estimate)
(29) **End**

V. SIMULATION RESULTS AND DISCUSSIONS

Computer simulations were carried out for QPSK, 16QAM and 64QAM in the 4×4 and the 8×8 MIMO systems. We estimated the transmitted signals using the proposed GS-F&B-LRA MMSE list detection.

Before calculating BERs for the proposed detection, we first determine the suitable value of δ in Table I and the suitable number of iterations I in Table III. After that, we analyze the BER performances and the computational complexity.

A. Suitable Values of Factor δ and of Number of Iterations I

We here determine the suitable values of δ and the suitable number of I for both the conventional and the proposed detections in the 4×4 and the 8×8 MIMO systems. Although the

optimum value of δ in terms of achieving low BER is dependent on E_b/N_0, we look for suitable value of δ that should achieve BER of 10^{-4}–10^{-5} at the lowest E_b/N_0. Then δ becomes optimum at BER≈10^{-4}–10^{-5}.

Figs. 1 (a), (b) and (c) show the δ vs. BER characteristics for various values of I, and the δ vs. the number of swapping times characteristics for QPSK, 16QAM and 64QAM at E_b/N_0 of 15dB, 20dB and 25dB over the 4×4 MIMO channel, respectively. Figs. 1 (d), (e) and (f) show those two characteristics for QPSK, 16QAM and 64QAM at E_b/N_0 of 11dB, 16dB and 21dB over the 8×8 MIMO channel, respectively.

Figs. 2 (a), (b) and (c) show the number of iterations I vs. BER characteristics for the proposed detection for QPSK, 16QAM and 64QAM at E_b/N_0 of 15dB, 20dB and 25dB over the 4×4 MIMO channel, respectively. Figs. 2 (d), (e) and (f) show those characteristics for the proposed detection for QPSK, 16QAM and 64QAM at E_b/N_0 of 11dB, 16dB and 21dB over the 8×8 MIMO channel, respectively. Table IV summarizes the suitable values of δ and those of I for the three modulation types in both the 4×4 and the 8×8 MIMO systems.

Remark that the parameter $j \in \{1,2\}$ achieves good BERs for the 4×4 MIMO system, while the parameter $j \in [1,4]$ is necessary to achieve good BERs for the 8×8 MIMO system.

TABLE IV
SUITABLE VALUES OF δ AND I

		QPSK	16QAM	64QAM
Conventional detection	4×4 MIMO	δ=0.75	δ=0.75	δ=0.75
	8×8 MIMO	δ=0.75	δ=0.75	δ=0.75
Proposed detection	4×4 MIMO: $j \in \{1,2\}$	δ=0 I=0	δ=0.4 I=1	δ=0.4 I=1
	8×8 MIMO: $j \in [1,4]$	δ=0 I=1	δ=0.75 I=4	δ=0.75 I=6

B. BER Performances

Figs. 3 (a)–(f) show the E_b/N_0 vs. BER characteristics for QPSK, 16QAM and 64QAM in the 4×4 and the 8×8 MIMO systems, setting δ shown in Table IV. In each figure, BER curves with legends (1) and (2) are derived using the conventional and the proposed detections, respectively.

Figs. 3 (a), (b) and (c) show the BER characteristics for QPSK, 16QAM and 64QAM in the 4×4 MIMO system, respectively. BER curve (2) for QPSK agreed and those for 16QAM and 64QAM almost agreed with the BER curves for the ML detection. As seen in Figs. 3 (b) and (c), the BER slopes are as steep as those for the ML detection. Hence we can obtain the same BER as that for the ML detection in the high E_b/N_0 region by increasing the transmit signal energy by 0.1dB and 0.3dB for 16QAM and 64QAM, respectively.

Figs. 3 (d), (e) and (f) show the BER characteristics for QPSK, 16QAM and 64QAM in the 8×8 MIMO system, respectively. BER curve (2) for QPSK agreed and those for 16QAM and 64QAM almost agreed with the BER curves for the ML detection. As seen in Figs. 3 (e) and (f), the BER slopes are as steep as those for the ML detection. Hence we can obtain the same BER as that for the ML detection in the high E_b/N_0 region by increasing the transmit signal energy by 0.1dB and 0.4dB for 16QAM and 64QAM, respectively.

As a consequence, the proposed detection dramatically improves the BER performances, which achieves near-ML BER performances, in particular, for the 8×8 MIMO system.

C. Computational Complexity Analysis

We count up the number of calculations of the multiplication of two complex values in Tables I–III and the number of those calculations of eqs. (5), (11) and (17) and their related calculations, since those calculations dominantly contribute to the computational complexity.

In Table I, the number of calculations of $\hat{\mathbf{h}}_q^{\mathrm{H}}\mathbf{h}_p$ in step (4) and of $\hat{\mathbf{h}}_q^{\mathrm{H}}\hat{\mathbf{h}}_p$ in step (9) at p with $q \in [1, p-1]$ is a total of $2(p-1)$. Hence, with weak reduction, the total number of those calculations over $p \in [2,M]$ is $\sum_{p=2}^{M} 2(p-1) = M(M-1)$. Since both $\hat{\mathbf{h}}_p$ and $\mathbf{h}_p$ have $2M$ entries each, we have $2M \cdot M(M-1)$ $(=2M^2(M-1))$ multiplications for the above calculations. The number of divisions in both steps (4) and (9) is $M(M-1)$. For the squared norms $\|\hat{\mathbf{h}}_q\|^2$'s in steps (4) and (9) at p with $q \in [1, p-1]$, we need to calculate only $\|\hat{\mathbf{h}}_{p-1}\|^2$ at p, since the other $\|\hat{\mathbf{h}}_q\|^2$'s for $q \in [1, p-2]$ have already been calculated before p in the for-loop of p. Hence the total number of multiplications for $\|\hat{\mathbf{h}}_{p-1}\|^2$ at p is $2M$. With weak reduction, we have a total of $2M(M-1)$ multiplications for $\|\hat{\mathbf{h}}_{p-1}\|^2$ over $p \in [2,M]$. The number of calculations in both steps (5) and (10) at p with $q \in [1, p-1]$ is a total of $3(p-1)$. With weak reduction, we have a total of $2M\sum_{p=2}^{M} 3(p-1) (= 3M^2(M-1))$ multiplications in steps (5) and (10) over $p \in [2,M]$.

If a column-swapping occurs at p, then p goes back to $(p-1)$. The number of calculations of both $\hat{\mathbf{h}}_q^{\mathrm{H}}\mathbf{h}_p$ in step (4) and $\hat{\mathbf{h}}_q^{\mathrm{H}}\hat{\mathbf{h}}_p$ in step (9) at p and the number of divisions of them by $\|\mathbf{h}_q\|^2$ at p are $2(p-1)$ each, and those at $(p-1)$ are $2(p-2)$ each. Hence we have $2M \cdot \{2(p-1)+2(p-2)\} (=4M(2p-3))$ multiplications and $\{2(p-1)+2(p-2)\} (=2(2p-3))$ divisions due to the column-swapping at p. The number of multiplications in both steps (5) and (10) at both p and $(p-1)$ is a total of $2M\{3(p-1)+3(p-2)\}=6M(2p-3)$. Similarly, the number of multiplications for $\|\hat{\mathbf{h}}_{p-1}\|^2$ at p and for $\|\hat{\mathbf{h}}_{p-2}\|^2$ at $(p-1)$ in both steps (4) and (9) is a total of $2M \cdot 2 = 4M$. Let a be the average column-swapping times. Assuming that the column-swapping occurs uniformly with respect to p, the total number of multiplications in Table I is

$$\begin{aligned} A_{\mathrm{I}}(M,a) &= 4M(M-1+2a) + (M-1)(2M^2+M+2M+3M^2) \\ &\quad + \tfrac{a}{M-1}\textstyle\sum_{p=2}^{M}\{(4M+2+6M)(2p-3)+4M\} \\ &= M(M-1)(5M+7) + 2a(5M^2+2M-1) \end{aligned}$$

on average. Here the term $4M(M-1+2a)$ is the number of multiplications for the squared norm of the right hand side of the inequality in step (12). Note that the left hand side $\|\hat{\mathbf{h}}_{p-1}\|^2$ at step (12) has already been calculated at step (4). Also note that the column-swapping practically more often occurs at the smaller p than at the larger p. Therefore the actual number of multiplications in Table I should be smaller than $A_{\mathrm{I}}(M,a)$.

In Table II, the column vectors of $\mathbf{H}'$ are weakly reduced. Hence the total number of multiplications for $\hat{\mathbf{h}}_q^{\mathrm{H}}\hat{\mathbf{h}}_p$ and that for $\|\hat{\mathbf{h}}_q\|^2$ at step (4) over $p \in [2,M]$ are $M^2(M-1)$ and $2M(M-1)$, respectively. The number of divisions in step (4) is

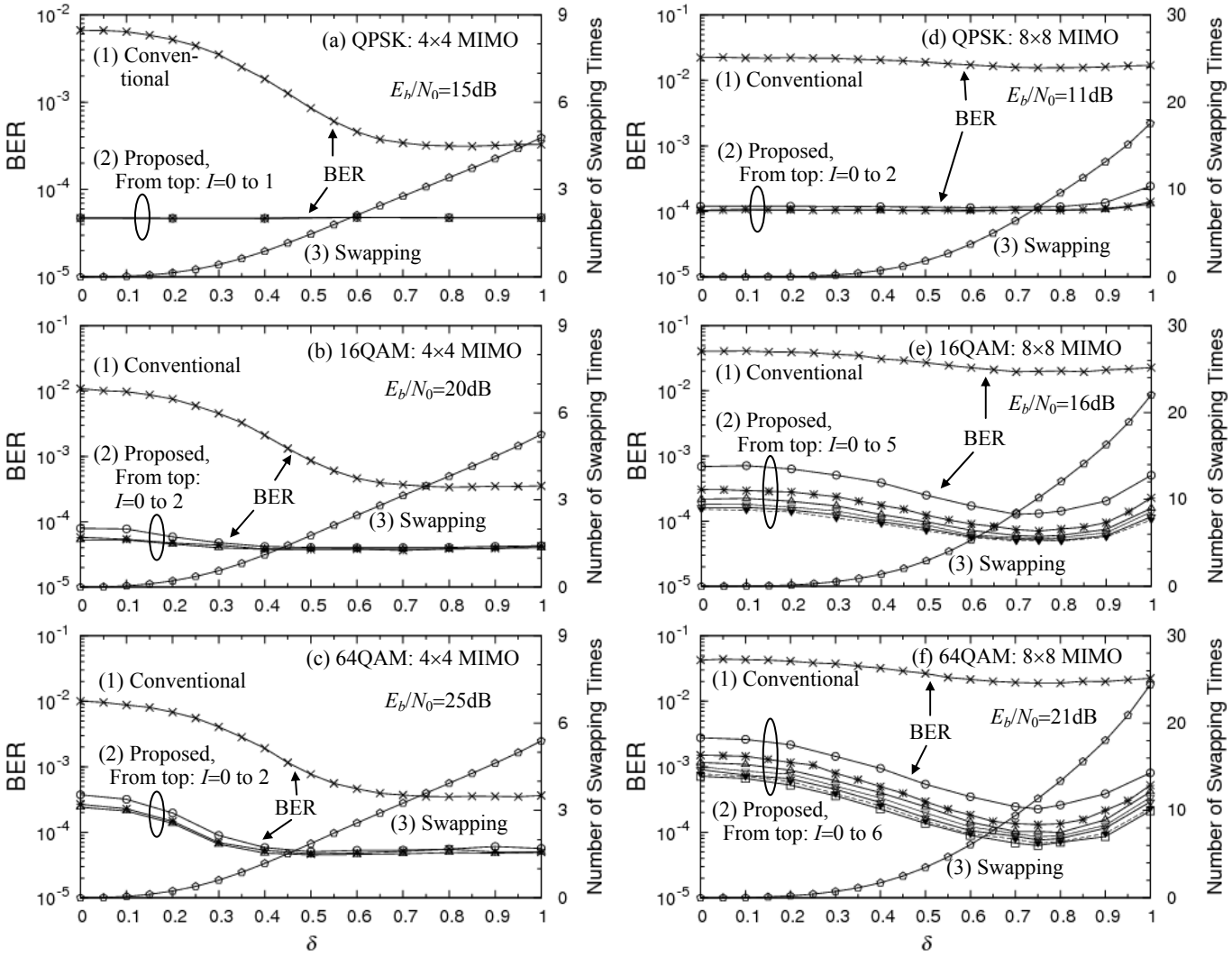

Fig. 1- The δ vs. BER characteristics and the δ vs. the number of swapping times characteristics; (a)–(c) 4×4 MIMO, (d)–(f) 8×8 MIMO; (a) QPSK at E_b/N_0=15dB, (b) 16QAM at E_b/N_0=20dB, (c) 64QAM at E_b/N_0=25dB, (d) QPSK at E_b/N_0=11dB, (e) 16QAM at E_b/N_0=16dB, (f) 64QAM at E_b/N_0=21dB; Curves (1) and (2) are BERs for the conventional and the proposed detections, respectively. Curves (3) are the number of swapping times.

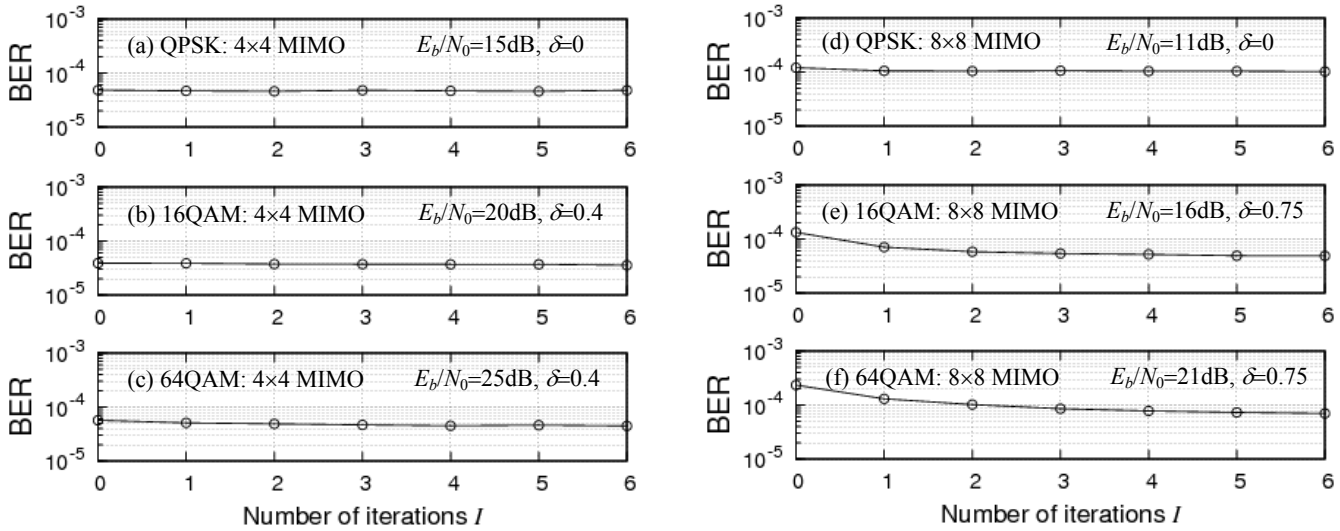

Fig. 2- The number of iterations I vs. BER characteristics for the proposed detection; (a)–(c) 4×4 MIMO, (d)–(f) 8×8 MIMO; (a) QPSK at E_b/N_0=15dB with δ=0, (b) 16QAM at E_b/N_0=20dB with δ=0.4. (c) 64QAM at E_b/N_0=25dB with δ=0.4, (d) QPSK at E_b/N_0=11dB with δ=0, (e) 16QAM at E_b/N_0=16dB with δ=0.75. (f) 64QAM at E_b/N_0=21dB with δ=0.75.

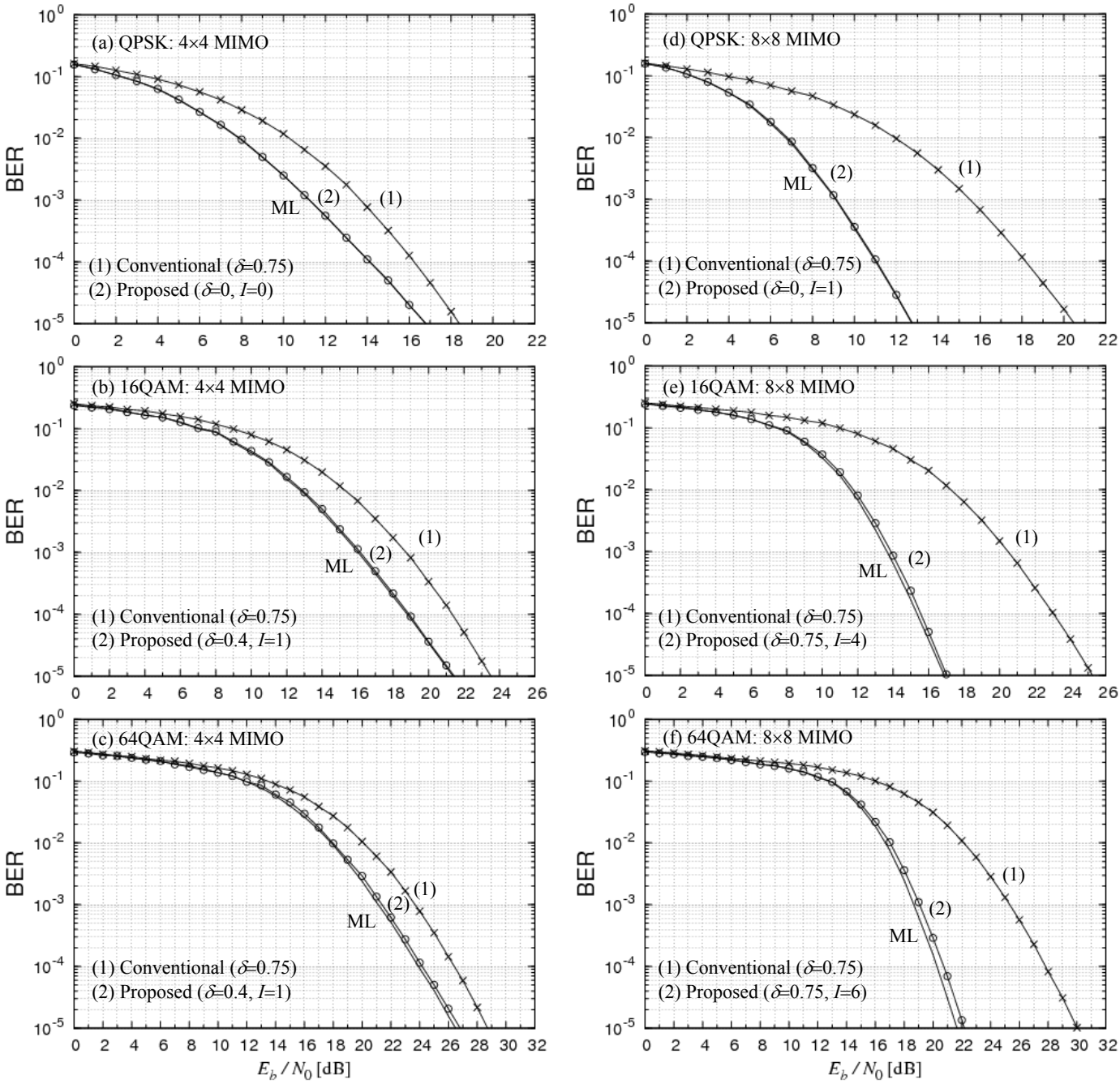

Fig. 3- The E_b/N_0 vs. BER characteristics; (a)–(c) 4×4 MIMO, (d)–(f) 8×8 MIMO; (a) QPSK, (b) 16QAM, (c) 64QAM, (d) QPSK, (e) 16QAM, (f) 64QAM; BER curves (1) and (2) are derived using the conventional and the proposed detections, respectively.

$M(M-1)/2$. The total number of multiplications in step (5) is $2M^2(M-1)$. As a result, the total number of multiplications in Table II is $A_{\mathrm{II}}(M) = (M-1)(M^2 + 2M + \frac{1}{2}M + 2M^2)$.

To derive the inverse of an $M\times M$ matrix, we used the LU decomposition method, which requires $4M^3/3$ multiplications [11]. Hence, the calculation of $(\mathbf{H}^{\mathrm{H}}\mathbf{H}+\rho\mathbf{I}_M)^{-1}\mathbf{H}^{\mathrm{H}}\mathbf{y}$ in (5) requires the number of multiplications of $S(M) = \frac{1}{2}M^2(M+1) + \frac{4}{3}M^3 + 2M^2$. Both $\hat{\mathbf{s}}'^{(j)} = \mathbf{T}^{(j)}\hat{\mathbf{v}}^{(j)}$ in (17) and $\tilde{\mathbf{v}}^{(j)} = \mathbf{T}^{(j)-1}\tilde{\mathbf{s}}$ require the total number of multiplications of $T(M) = 2M^2 + \frac{4}{3}M^3$ for each j. Both $\hat{\underset{\sim}{\mathbf{T}}}^{(j,k)} = \mathbf{T}^{(j)}\hat{\mathbf{T}}^{(j,k)}$ and $\tilde{\mathbf{u}}^{(j,k)} = \hat{\underset{\sim}{\mathbf{T}}}^{(j,k)-1}\tilde{\mathbf{s}}$ in (11) require the total number of multiplications of $U(M) = \frac{1}{2}M^2(M+1) + (\frac{4}{3}M^3 + M^2)$ for each j and k.

In the proposed detection algorithm of Table III, the equations in steps (11), (21) and (25) hold in high probabilities of more than 80, 95 and 99 percent at BER≈10^{-5}, respectively. The equation in step (17) holds in high probabilities of more than 97 and 98 percent for i=1 and i≥2, respectively. Hence the steps (12), (18), (22) and (26) are seldom needed to calculate. This fact implies that they negligibly contribute to the computational complexity.

Since $\hat{\mathbf{T}}^{(j,k)-1}$ has already been derived, the calculation for $\hat{\underset{\sim}{\mathbf{T}}}^{(j,k)-1}\hat{\mathbf{s}}'^{\{i\}}$ in step (6) requires M^2 multiplications for each j, k and i. For the 4×4 MIMO system with $j\in\{1,2\}$, $k\in[1,4]$, the $\hat{\underset{\sim}{\mathbf{T}}}^{(j,k)-1}\hat{\mathbf{s}}'^{\{i\}}$ should be calculated 8(=2M) times for each i. For

the 8×8 MIMO system with $\{j|k\} \in [1,4]$, it should be calculated 16(=2M) times for each i. Hence, the total number of multiplications for $\hat{\mathbf{T}}^{(j,k)-1}\hat{\mathbf{s}}'^{\{i\}}$ is $M^2 \cdot 2M(I+1)=2M^3(I+1)$. Similarly, $\hat{\mathbf{T}}^{(j,k)}\hat{\mathbf{u}}^{(0,j,k)}$ in step (7) and $\hat{\mathbf{T}}^{(j,k)}\hat{\mathbf{u}}^{(p,j,k)}$ in step (10) require $2M^3(I+1)$ and $2M^4(I+1)$ multiplications, respectively. As a result, the total number of multiplications in Table III is $A_{\mathrm{III}}(M,I)=(4M^3+2M^4)(I+1)$. It should be noted that all the calculations in steps (6), (7) and (10) are not done since the process skips out of the for-loop of i at $i<I$ in step (17). This process decreases the iteration times. Hence the actual number of multiplications in Table III is smaller than $A_{\mathrm{III}}(M,I)$.

We first count up the number of calculations for 64QAM in the 4×4 MIMO system, where M=4. As we set δ=0.75 for the conventional detection in Table IV, the average swapping times are a=3.6 at E_b/N_0=25dB from Fig. 1 (c). Hence the total number of multiplications is $N_c \equiv A_{\mathrm{I}}(4,3.6)+S(4)+T(4)=1225$ for the conventional detection.

For the proposed detection, we set δ=0.4 and I=1 for 64QAM in Table IV. From Fig. 1 (c), the average swapping times are a=1.1 at E_b/N_0=25dB. As we chose $j \in \{1,2\}$ for the 4×4 MIMO system, the LLL algorithm is used twice. Hence the total number of multiplications in Table I is $2A_{\mathrm{I}}(4,1.1)$. We further reduced the columns of $\overline{\mathbf{H}}'^{(j,k)}: j \in \{1,2\}$, $k \in [1,4]$, eight times using Table II. Hence the number of multiplications in Table II is $8A_{\mathrm{II}}(4)$. The number of multiplications in Table III is $A_{\mathrm{III}}(4,1)$, where the skipping-out process at step (17) in the for-loop of i is not taken into consideration. The number of multiplications of (5), (11), (17), $\mathbf{T}^{(j)}\hat{\mathbf{T}}^{(j,k)}$ and $\mathbf{T}^{(j)-1}\tilde{\mathbf{s}}$ is a total of $S(4)+2T(4)+8U(4)$. As a result, the total number of multiplications for the proposed detection is $N_p \equiv 2A_{\mathrm{I}}(4,1.1)+8A_{\mathrm{II}}(4)+A_{\mathrm{III}}(4,1)+S(4)+2T(4)+8U(4)=5481$. Since N_p/N_c=4.5, the proposed detection has 4.5 times larger number of calculations than the conventional detection.

In the similar manner, we counted up the number of multiplications for the 8×8 MIMO system, where a=11.4 for δ=0.75 at E_b/N_0=21dB from Fig. 1 (f) with setting I=6 in Table IV. And it was found that the proposed detection has 12.9 times larger number of calculations than the conventional detection.

As a result, the computational complexity for the proposed detection is around 4.5 times and around 12.9 times larger than the conventional LRA MMSE detection in the 4×4 and the 8×8 MIMO systems, respectively.

VI. Conclusions

In this paper, we proposed an improved lattice-reduction aided MMSE list detector by combining the LLL algorithm and the Gram-Schmidt procedure. First we forward and backward reduced the column vectors of the extended channel matrix using the LLL algorithm to create two reduced channel matrices. In order to achieve more reliable estimate, we further created two more LLL-reduced channel matrices by rearranging the order of the columns of the extended channel matrix. Those LLL-reduced column vectors are forward and backward reduced using the GS procedure to create the column vectors purely orthogonal to one another. After that, we created eight or 16 estimates of the transmitted signal. Among them, we selected the most reliable estimate.

The proposed detector dramatically improved the BER performances for QPSK, 16QAM and 64QAM in both the 4×4 and 8×8 MIMO systems. It achieved near-ML BER performances. This is because the GS procedure creates the column vectors of the reduced channel matrix to be mutually purely orthogonal. Hence the decision boundary became the same as that of the ML detection.

As a consequence, the proposed detector is worthy for applying to both the 4×4 MIMO and the 8×8 MIMO systems.

References

[1] A. K. Lenstra, H. W. Lenstra, and L. Lovász, "Factoring polynomials with rational coefficients," *Math. Annalen*, Vol. 261, No. 4, pp. 515-534, Springer, Dec. 1982.

[2] T. D. Nguyen, X. N. Tran, and T. Fujino, "Layered error characteristics of lattice-reduction aided V-BLAST detectors," *IEICE Trans. on Fundamentals of Electron., Commun. and Computer Sciences,* Vol. E89-A, No. 10, pp. 2535-2542, Oct. 2006.

[3] D. Wübben, R. Böhnke, V. Kühn, and K. D. Kammeryer, "Near-maximum-likelihood detection of MIMO systems using MMSE-based lattice reduction," *IEEE Int. Conf. on Commun. (ICC'04)*, Vol. 2, June, 2004.

[4] X. Wang, Z. He, K. Niu, W. Wu, and X. Zhang, "An improved detection based on lattice reduction in MIMO systems," *IEEE Int. Symposium on Personal, Indoor and Mobile Radio Commun. (PIMRC'06)*, Sep. 2006.

[5] H. Yao and G. W. Wornel, "Lattice-reduction-aided detector for MIMO communication systems," *IEEE Global Commun. Conf. (Globecom'02)*, Vol. 1, pp. 424-428, Nov. 2002.

[6] K. L. Clarkson, W. Sweldons, and A. Zheng, "Fast multiple-antenna differential decoding," *IEEE Trans. Commun.,* Vol. 49, No. 2, pp. 253-261, Feb. 2001.

[7] C. Windpassinger and R. F. H. Fischer, "Low-complexity near-maximum-likelihood detection and precoding for MIMO systems using lattice reduction," *IEEE Inform. Theory Workshop*, France, 2003.

[8] H. Hassibi, "An efficient square-root algorithm for BLAST," *IEEE Int. Conf. on Acoustic, Speech, Signal Processing*, Istanbul, Turkey, pp. 5-9, 2000.

[9] T. Fujino and T. Shimokawa, "Combined forward and backward lattice-reduction aided MMSE detection in MIMO systems," *68th IEEE Vehicular Technol. Conf. (VTC'08-Fall)*, Calgary, Canada, Sep. 2008.

[10] T. Fujino, T. Shimokawa, and X. N. Tran, "Combined forward and backward lattice-reduction aided MMSE list detection," *IEEE 2008 Int. Conf. on Advanced Technol. for Commun. (ATC'08)*, Hanoi, Vietnam, Oct. 2008.

[11] Autar Kaw, *Introduction to matrix algebra,* Autarkaw.com, 2008, ISBN: 978-0-615-25126-4.